Lipoprotein-associated phospholipase A_2 (Lp-PLA_2) as a therapeutic target to prevent retinal vasopermeability during diabetes

Paul Canning [a], Bridget-Ann Kenny [b], Vivien Prise [a], Josephine Glenn [a], Mosharraf H. Sarker [b,c], Natalie Hudson [b], Martin Brandt [d], Francisco J. Lopez [e], David Gale [e], Philip J. Luthert [b], Peter Adamson [f,g], Patric Turowski[b,1,2],and Alan W. Stitt[a,1,2].

[a] Centre for Experimental Medicine, School of Medicine, Dentistry and Biomedical Science, Queen's University Belfast, Royal Victoria Hospital, Belfast, United Kingdom; [b] Department of Cell Biology, University College London Institute of Ophthalmology, London EC1V 9EL, United Kingdom; [c] School of Science &Engineering, Teesside University, Middlesbrough TS1 3BA, United Kingdom; [d] Platform Technology Sciences, GlaxoSmithKline, King of Prussia, PA 19406; [e] Ophthalmology Discovery Performance Unit, GlaxoSmithKline, King of Prussia, PA 19406; [f] Ophthalmology Discovery Performance Unit, GlaxoSmithKline, Stevenage, United Kingdom; and [g] Ocular Biology and Therapeutics, University College London Institute of Ophthalmology, London EC1V 9EL, United Kingdom.

Edited by Jian-xing Ma, University of Oklahoma Health Science Center, Oklahoma City, OK, and accepted by Editorial Board Member Jeremy Nathans May 6, 2016 (received for review July 22, 2015).

Footnotes

[1]P.T. and A.W.S. contributed equally to this work.

[2]To whom correspondence may be addressed. Email: a.stitt@qub.ac.uk or p.turowski@ucl.ac.uk.

Author contributions: F.J.L., P.A., P.T., and A.W.S. designed research; P.C., B.-A.K., V.P., J.G., M.H.S., N.H., M.B., D.G., P.J.L., P.T., and A.W.S. performed research; F.J.L. contributed new reagents/analytic tools; P.C., B.-A.K., J.G., D.G., and P.T. analyzed data; and P.C., P.A., P.T., and A.W.S. wrote the paper.

Conflict of interest statement: The authors M.B., F.J.L., D.G., and P.A. are (or have been) employed by GlaxoSmithKline. The funding of this research has been through a grant provided by GlaxoSmithKline.

This article is a PNAS Direct Submission. J.-x.M. is a guest editor invited by the Editorial Board.

This article contains supporting information online at www.pnas.org/lookup/suppl/doi:10.1073/pnas.1514213113/-/DCSupplemental.

Significance

Breakdown of the blood–retinal barrier (BRB) is central to diabetic macular edema (DME). Here, we demonstrate that lipoprotein-associated phospholipase A_2 (Lp-PLA_2) plays a critical role in diabetes-related retinal vasopermeability, a response that is mediated by lysophosphatidylcholine (LPC). Because neutralization of VEGF is the current gold-standard treatment for DME, we assessed suboptimal systemic treatment of an Lp-PLA_2 inhibitor alongside a suboptimal intravitreal injection with a rat-specific VEGF antibody and demonstrated that protection against diabetes-mediated retinal vasopermeability was additive. We have also shown a coalescence of the LPC and VEGF pathways in retinal vascular endothelium via a common VEGF receptor 2-mediated mechanism. Alongside currently administered anti-VEGF agents, Lp-PLA_2 may be a useful therapeutic target for DME.

Abstract

Lipoprotein-associated phospholipase A_2 (Lp-PLA_2) hydrolyses oxidized low-density lipoproteins into proinflammatory products, which can have detrimental effects on vascular function. As a specific inhibitor of Lp-PLA_2, darapladib has been shown to be protective against atherogenesis and vascular leakage in diabetic and hypercholesterolemic animal models. This study has investigated whether Lp-PLA_2 and its major enzymatic product, lysophosphatidylcholine (LPC), are involved in blood–retinal barrier (BRB) damage during diabetic retinopathy. We assessed BRB protection in diabetic rats through use of species-specific analogs of darapladib. Systemic Lp-PLA_2 inhibition using SB-435495 at 10 mg/kg (i.p.) effectively suppressed BRB breakdown in streptozotocin-diabetic Brown Norway rats. This inhibitory effect was comparable to intravitreal VEGF neutralization, and the protection against BRB dysfunction was additive when both targets were inhibited simultaneously. Mechanistic studies in primary brain and retinal microvascular endothelial cells, as well as occluded rat pial microvessels, showed that luminal but not abluminal LPC potently induced permeability, and that this required signaling by the VEGF receptor 2 (VEGFR2). Taken together, this study demonstrates that Lp-PLA_2 inhibition can effectively prevent diabetes-mediated BRB dysfunction and that LPC impacts on the retinal vascular endothelium to induce vasopermeability via VEGFR2. Thus, Lp-PLA_2 may be a useful therapeutic target for patients with diabetic macular edema (DME), perhaps in combination with currently administered anti-VEGF agents.

diabetic retinopathy ,VEGF signaling, lysophosphatidylcholine, blood–retinal barrier, lipoprotein-associated phospholipase A2

Breakdown of the blood–retinal barrier (BRB) is a significant pathophysiological event during diabetic retinopathy (DR). Leakage of plasma proteins and lipids into the neuropile form exudates, whereas excessive vasopermeability can lead to diabetic macular edema (DME), which is a major cause of vision loss (1). Both DME in patients and BRB dysfunction in animal models have been linked to inflammatory processes, endothelial dysfunction, and compromise of normal neuroglial–vascular interactions (2). A number of therapeutic options are available to treat DME. Laser photocoagulation is effective in slowing the progression of DME; however, it carries risk of serious adverse side effects including visual field defects, retinal scarring, and foveal burns. Intravitreal injection of antiinflammatory corticosteroids has proven value, but this intervention also carries significant side effects including cataract formation and elevated intraocular pressure. More recently, neutralization of vascular endothelial growth factor (VEGF) in the retina has become a mainstream treatment of DME (3) although this is not effective for all DME patients (4). Moreover, repeated intravitreal injections can result in some patients becoming refractory to VEGF blockade (5), which suggests that other mechanisms also drive vascular permeability during DME. Concerns have also been raised that targeting the VEGF pathway could inadvertently compromise retinal neuroglial and microvascular survival (6) although, thus far, no evidence of these outcomes have been observed in clinical trials of anti-VEGF for DME. Nevertheless there is a need for additional therapeutic approaches to treat DME, either alone or adjunctively with currently available therapeutics.

An alternative permeability-inducing agent in diabetic retina could be lysophosphatidylcholine (LPC), which is elevated in plasma of diabetic patients (7) and has demonstrated permeability-enhancing activity in cultured nonneural endothelial cells (ECs) (8). The principal enzyme responsible for the production of LPC is a calcium-independent phospholipase A_2 called lipoprotein-associated phospholipase A_2 (Lp-PLA_2) (also known as platelet-activating factor acetylhydrolase or type VIIA PLA_2). Lp-PLA_2 can elicit a broad range of proinflammatory and proapoptotic effects in blood vessels related to its hydrolysis of modified polyunsaturated fatty acids within oxidized low-density lipoprotein (oxLDL) into LPC and oxidized nonesterified fatty acids (OxNEFA) (9). Elevated Lp-PLA_2 has been proposed as a predictive biomarker in stroke (10), atherosclerosis (11), and coronary heart disease (12). Macrophages and other proinflammatory cells are a primary source of Lp-PLA_2 in the systemic circulation (13), although endothelial cells also express this enzyme (14).

Darapladib, a specific inhibitor of Lp-PLA_2, has been shown to reduce atherosclerosis in both diabetic/hypercholesterolemic pigs (15) and ApoE-deficient mice (16). In diabetic/hypercholesterolemic pigs, darapladib protected against blood–brain barrier (BBB) dysfunction and vascular permeability (17). Darapladib has been studied in nearly 16,000 patients with coronary heart disease, and approximately one-third of this study population had diabetes mellitus (18). In a further study, a 3-month daily treatment with 160 mg of darapladib orally showed reduction of DME and an improvement in visual acuity in patients (19). These observations suggest that Lp-PLA_2 and its mechanism of action warrant further investigation in the context of DR. In this study, we have studied the inhibition of Lp-PLA_2 in diabetic rats with regards to BRB function and assessed the effect of LPC on neural microvascular endothelial cells. We show inhibition of Lp-PLA_2 was effective in reducing diabetes-induced retinal vasopermeability and that the effect of this inhibition was additive with VEGF neutralization, suggesting this enzyme could be an efficacious therapeutic target for DME, either alone or in combination with anti-VEGF therapeutics.

Results

Enhanced Lp-PLA_2 Activity During Diabetes Can Be Inhibited by Using SB435495.

Diabetes induction in Brown Norway (BN) rats resulted in significant hyperglycemia and weight loss, whereas treatment with SB435495, a rodent-specific analog of darapladib, had no effect on these parameters (Fig. S1 *A* and *B*). SB435495 inhibited Lp-PLA_2 in BN rat plasma with an IC_{50} of 8.8 ± 1.3 nM (Fig. 1*A*). Dosing of diabetic BN rats at 0.25, 1, 5, and 10 mg/kg SB435495 for 28 d reduced plasma Lp-PLA_2 activity levels to 72.8%, 57.5%, 33.5%, and 19.1%, respectively, compared with Lp-PLA_2 activity measured in plasma collected from rats before treatment ($P < 0.0001$) (Fig. 1*B*). This inhibition corresponded to SB435495 levels that accumulated in the plasma ($P < 0.001$) (Fig. 1*C*). Lp-PLA_2 activity was also measured in nondiabetic control and diabetic BN rat plasma collected at day 0 (before placebo administration) and day 28 of diabetes (after daily placebo administration). Lp-PLA_2 activity was elevated by approximately threefold in the plasma of diabetic rats

compared with that of nondiabetic controls ($P < 0.0001$) (Fig. 1*D*). Enhanced Lp-PLA$_2$ activity in diabetic BN rats was sustained for the 28-d duration of the experiment.

Lp-PLA$_2$ Inhibition Limits Diabetes-Induced Retinal Vasopermeability.

BRB integrity was quantified by measuring Evans blue extravasation in the retinae of BN rats that had been diabetic for 4 wk. Diabetes led to a significant retinal vasopermeability in BN rats compared with nondiabetic controls [nondiabetic control (NDB CON) mean = 2.291 vs. diabetic (DB) + placebo mean = 4.160 $\mu L \cdot g^{-1} \cdot h^{-1}$] (Fig. 2*A*), and this result is comparable to what has been shown in other studies using BN rats for this diabetes-duration time frame (20). SB435495 treatment at 10 mg/kg significantly attenuated diabetes-induced retinal vasopermeability ($P < 0.002$) (Fig. 2*A*).

As an additional approach to the Evans blue method, we analyzed histological aspects of diabetes-induced vasopermeability in BN rats using retinal sections from each treatment group stained for albumin extravasation from isolectin B4-stained retinal blood vessels. Quantification of albumin immunoreactivity revealed a significant increase in diabetic retina and a nearly complete reversal to control levels following treatment with 10 mg/kg SB435495 ($P < 0.0001$) (Fig. 2*B*). In control animals, albumin staining was confined to lectin-positive vessel structures (Fig. 2 *C*, *i*), whereas sections from diabetic animals displayed many areas of extravascular albumin staining throughout the retinal neuropile, indicative of enhanced vascular leakage (Fig. 2 *C*, *ii* and Figs. S2 and S3). This albumin leakage was focal in nature and mostly occurred in the vicinity of vessels that appeared strongly dilated. Treatment with SB435495 (10 mg/kg) resulted in a strong reduction of these areas of albumin leakage, to levels similar to that observed in the nondiabetic control rat retina (Fig. 2 *C*, *iii* vs. Fig. 2 *C*, *i*). This morphological approach in an additional group of animals using an independent vasopermeability detection method corroborates our Evans Blue data.

We also tested the effect of SB435495 on diabetes-induced vasopermeability in a therapeutic setting. For this experiment, BN rats that had been diabetic for 28 d were treated with placebo or SB435495 by a daily 10 mg/kg i.p. injection for an additional 28 d. Retinal vasopermeability was assessed by analysis of albumin immunoreactivity in retinal sections. Compared with the nondiabetic controls, vehicle-treated diabetic animals displayed clear extravasation of albumin (Fig. S3). In contrast, the SB435495-treated animals demonstrated a clear effect in limiting extravasation of albumin at the end of the treatment period, indicating that both preventive and therapeutic Lp-PLA$_2$ inhibition by SB435495 effectively reduced retinal vascular leakage in diabetic BN rats.

Synergistic Effect of VEGF and Lp-PLA$_2$ Neutralization on BRB Function.

We next investigated how Lp-PLA$_2$ inhibition interacted with blockade of the VEGF signaling axis. Diabetic BN rats were treated with either control IgG antibodies, or the anti-rat VEGF neutralizing antibody DMS1529, either alone or in combination with SB435495 treatment. Control IgG antibody and VEGF neutralizing antibodies were administered as 1-μL intravitreal injections in both eyes at day 26 of diabetes. SB435495 was administered i.p. for 28 d and retinal vasopermeability assessed by Evans blue assay. Retinal vasopermeability was significantly elevated in diabetic/IgG-treated rats compared with nondiabetic controls ($P < 0.05$) (Fig. 3). Intravitreal injection of diabetic rats with anti-VEGF antibody (0.5 mg/mL) had no statistically significant effect on vasopermeability, nor did SB435495 at a dose of 5 mg/kg in combination with IgG (Fig. 3*B*). In contrast, higher concentrations of anti-VEGF antibody (1 mg/mL) or SB435495 (10 mg/kg) were highly effective in suppressing diabetes-induced vasopermeability. When suboptimal intravitreal anti-VEGF injection (0.5 mg/mL) was combined with suboptimal regimen of SB435495 (5 mg/kg), there was a significant reduction in retinal vasopermeability compared with suboptimal monotherapy ($P < 0.05$).

LPC-Induced Vasopermeability in Neural Microvascular Endothelium.

Lp-PLA$_2$ enzymatic activity produces LPC, which induces vasopermeability in cultured dermal and lung microvascular endothelial cells (MVECs) (8). To understand the action of diabetes-induced Lp-PLA$_2$ activity, we investigated the effect of LPC on brain and retinal endothelium. MVECs with highly preserved interendothelial junctions, apico-basal polarity, and barrier properties (21) were isolated from rat brain or retinae. Brain MVECs

were readily isolatable and used at passage 0, whereas retinal MVECs were further subcultured by one round of trypsinization. Treatment of brain MVECs with LPC caused a significantly enhanced flux of 4-kDa FITC-dextran in a dose-dependent manner ($P < 0.05$–0.001) (Fig. 4*A*) and transiently reduced transendothelial electrical resistance (TEER) ($P < 0.0001$) (Fig. 4*B*), indicating that paracellular permeability was induced. Maximal disruption of the barrier was evident after less than 10 min of LPC addition. In retinal MVECs (Fig. 4*C*), LPC also induced a transient drop in TEER, albeit of less potency and at slightly later time (approximately 15 min) ($P < 0.05$) compared with the brain MVECs, which possibly reflected the effect of passaging of the retinal MVECs (21).

LPC also induced vasopermeability in occluded rat pial microvessels in vivo. Significantly, it was only effective when administered from the luminal (blood) but not the abluminal (tissue) side ($P < 0.05$) (Fig. 4 *D*–*G*). Similarly cultured brain MVECs responded with enhanced flux in response to apically but not basally applied LPC (Fig. 4 *H*), indicating that directionality was brought about by the endothelium itself.

In the retina and the brain, VEGF-A induces endothelial permeability via activation of p38 (21); therefore, the relationship between LPC and this VEGF-induced signaling pathway in MVECs was assessed. LPC treatment of the retinal MVEC line PT2 (described in Figs. S4 and S5) led to enhanced phosphorylation of p38 within 5 min ($P < 0.005$) (Fig. 5*A*). LPC also led to phosphorylation of the VEGFR2 on Y1175, which was comparable to that induced by VEGF-A itself ($P < 0.01$) (Fig. 5*B*). This phosphorylation was suppressed by preincubation with the VEGFR2-specific kinase antagonist SU1498, indicating potential transactivation. SU1498 also inhibited LPC-induced reduction of TEER in brain and retinal MVECs ($P < 0.01$) as did another VEGFR2 kinase antagonist, PTK/ZK, with different overall specificity ($P < 0.001$) (Fig. 5 *C* and *D*). SU1498 also inhibited LPC-induced flux in brain MVECs in vitro ($P < 0.01$) (Fig. 5*E*). However, neutralization of VEGF-A using either the antibody DMS1529 or aflibercept (EYELEA) failed to affect LPC-induced flux across brain MVECs (Fig. 5 *E* and *F*), indicating that VEGF secretion was not responsible for VEGFR2 transactivation. To confirm the definitive involvement of VEGFR2 in LPC-induced permeability, electrical barrier breakdown was measured in primary brain MVECs infected with shRNA-coding adenovirus 48 h before LPC addition (Fig. 5*G*). Infection with a virus targeting VEGFR1 had no effect on LPC-induced TEER reduction. Significantly, infection with a virus that led to knockdown of VEGFR2, attenuated LPC-induced barrier breakdown ($P < 0.01$), indicating that LPC requires VEGFR2 kinase activity to induce vasopermeability. The requirement of VEGFR2 for LPC-induced permeability was also corroborated in pial microvessels in vivo, where SU1498 completely suppressed the permeability response to LPC (Fig. 5*H*).

Discussion

Lp-PLA_2 has been proposed as a circulating biomarker for inflammatory disease, whereas increased activity of Lp-PLA_2 has been linked to vascular dysfunction (22). The pathogenic role of Lp-PLA_2 has been mostly focused on the macrovasculature and atherosclerosis, but the current study indicates that Lp-PLA_2 could also play an important role in retinal microvascular pathology during diabetes. During diabetes oxLDL is specifically found at sites of retinal vascular and glial cell damage (23) and this association could be mediated, at least in part, by abnormal Lp-PLA_2 activity in the blood stream or even by the retinal vasculature itself. Lp-PLA_2-associated damage to the vasculature is mediated by its bioactive reaction products, LPC and OxNEFA, which promote prooxidant and proinflammatory activity on the endothelium (24) and induce vasopermeability (8). LPC levels in plasma and Lp-PLA_2 activity have been reported to be elevated in diabetic patients (7). The current study has also demonstrated a significant increase in Lp-PLA_2 activity in serum from diabetic rats.

DME in patients usually takes years to manifest, although comparatively short-term diabetes in rodents has been used as a model system to study retinal vasopermeability and BRB compromise as retinopathy progresses (25). For the current study, the BN rat model was chosen because this strain demonstrates a robust and sustained breakdown of the BRB when rendered diabetic, a response that is clear after 4 wk and beyond (20). Evan's blue extraction allowed quantitative measure of BRB damage in this model, whereas immunohistochemistry demonstrated the focal nature of vasopermeability in the diabetic BN rats, which is related to endothelial dysfunction. Darapladib is a selective inhibitor of Lp-PLA_2 with demonstrable efficacy against atherogenesis in preclinical models (15). In diabetic and hypercholesterolemic pigs, darapladib prevents leakage of circulating IgG into the brain parenchyma, suggesting a protective effect of BBB function (17) while some pyrimidone derivatives have been shown to inhibit Lp-PLA_2 activity and reduce morphological

changes to retinal layers in diabetic rats (26). However, the consequence or mechanism of Lp-PLA_2 inhibition on retinal vascular permeability has not yet been investigated. The data presented herein show amelioration of a similar BRB dysfunction in diabetic rats by using the darapladib analog SB435495 and supports the modulatory role of Lp-PLA_2 in retinal vasopermeability. Additional data generated in Lp-PLA_2-suppressed rabbits indicated that the lipase did not affect the vasopermeability pathway directly, at least not that induced by VEGF (Fig. S4 and Table S1). Thus, it is likely that Lp-PLA_2 affected retinal vasopermeability in diabetes through its plasma oxLDL reaction product, LPC.

We confirmed the permeability-inducing effect of LPC in microvascular endothelium of neural origin in vitro and in vivo. Brain and retinal microvascular endothelial cells showed significant dose-dependent permeability responses to LPC, and this response was also true in an in vivo model of occluded pial microvessels. The precise nature of the endothelial LPC receptor is unknown, but this lipid has been reported to act as a multiactivity ligand, binding a number of proteins including: the CD36 scavenger receptor, Toll-like receptors (TLR4 and TLR2), and also the lectin-like oxLDL receptor-1 (LOX-1), after which it triggers a range of prooxidant and proinflammatory pathways (27⇓–29). Studies also implicate G protein-coupled receptors in mediating LPC function (30). Interestingly, LPC only exerted this action from the luminal vessel side or the apical side of the endothelium, and indicated that elevated plasma LPC in diabetes can act on the luminal side of the endothelium to induce vascular leakage. Interestingly, this effect is opposite to what is observed for VEGF-A (21). In agreement to others (31), we also found that LPC transactivated VEGFR2, and that this transactivation, which did not require VEGF, was a key signaling pathway in the induction of LPC-induced permeability both in vitro and in vivo. Transactivation of VEGFR2 may thus occur within the cell, possibly through reactive oxygen species (32). Taken together, our data lend further support to the central role of VEGFR2 and its kinase activity in VEGF-dependent and independent vascular permeability.

The role of VEGF in vasopermeability is well-established, and delivery of this growth factor into mammalian eyes can induce a transient but robust breakdown of the BRB (25), which may be mediated by alteration of paracellular tight-junction integrity (33) and induction of a transcellular vesicular pathway (34). The importance of VEGF in DME has found ultimate credence by the observation that many patients' retinal edema and vision impairment improves significantly in response to regular intravitreal injections of anti-VEGFs, such as ranibizumab (35). However, at least 50% of patients do not clinically respond, or respond in a delayed manner, to VEGF neutralization, suggesting alternative permeability factors may be involved (2). Here, we propose Lp-PLA_2 activity and its plasma-borne reaction products may constitute another pathway to retinal vasopermeability. Indeed, a parallel prospective phase IIa study shows that darapladib, given over a 3-month period, leads to improvement in DME-associated vision loss and edema (19).

In diabetic BN rats, suboptimal SB435495 application combined with suboptimal VEGF neutralization (using DMS1529) led to effective suppression of retinal vasopermeability, suggesting that two partially independent but additive pathways were targeted. Importantly, our rabbit data showed that Lp-PLA_2 inhibition did not affect the VEGF-induced vasopermeability pathway, also underlining that these pathways are somewhat distinct. We also found that there was a coalescence of these two pathways because LPC-induced microvascular permeability in vitro and in vivo depended on VEGFR2 signaling. Further studies are needed to clarify the effect of Lp-PLA_2 products on the BRB microvasculature as well as LPC-induced endothelial signaling and its crosstalk with other permeability pathways. Importantly, data from the present study has identified Lp-PLA_2 as a valid VEGF-independent therapeutic target in DME, but also indicated that Lp-PLA_2 inhibition could be combined with that of VEGF. This finding opens the possibility of combination therapy with the benefits of use of lower drug dosages and lower potential toxicity.

Materials and Methods

Lp-PLA_2 Inhibition in Diabetic Rats and Prevention of Diabetes-Induced Retinal Vasopermeability.

All experiments using animals conformed to U.K. Home Office regulations. Furthermore, studies were carried out in accordance with the European Directive 86/609/EEC, the GlaxoSmithKline Policy on the Care, Welfare, and Treatment of Animals, and the Association for Research in Vision and Ophthalmology (ARVO) Statement on the Use of Animals in Ophthalmic and Vision Research. Diabetes was induced in male adult BN rats (20). For detailed protocols and assessment of diabetes status, refer to *SI Materials and Methods*. SB-435495 and SB-

568859 (GlaxoSmithKline) are potent and selective pharmacological inhibitors of Lp-PLA_2 in a variety of species (36, 37). Pharmacokinetic properties of SB-568859 were most applicable to studies in rabbits, whereas SB-435495 was best suited for studies in rats (38). Details of formulation, plasma drug levels, and enzymatic activity is available in *SI Materials and Methods*.

Diabetic rats were randomly assigned into groups receiving either a once-daily i.p. injection of placebo (vehicle) or once-daily dosing of SB435495 (dose range: 0.25–10 mg/kg). A control group of nondiabetic, age-matched rats received no treatment. After 28 d, animals were processed for analysis of retinal vasopermeability. In further studies where the effect of combination of anti-VEGF and SB435495 therapies on diabetes-induced retinal vasopermeability was studied, anti-VEGF or control antibodies were introduced by intravitreal injections in both eyes, at day 26 after initial SB435495 administration. Retinal vasopermeability indicating breakdown of the BRB was assessed by using the Evans blue assay as described (25). Additionally, albumin leakage into the retina was analyzed by using immunohistochemistry.

Vascular Permeability in MVECs and Pial Microvessels.

Primary MVECs were isolated from rat brains or retinae and grown as described (21). A stable rat retinal MVEC line (PT2) was also used to provide the larger cell quantities necessary for biochemical analyses (Fig. S5) (39). For some experiments, cells were infected with recombinant adenoviruses carrying small hairpin RNAs targeting either mouse or rat VEGFR1 or VEGFR2. LPC was diluted into PBS, which was supplemented with 0.1% fatty-acid free BSA and flux measurements performed as described by using 4-kDa FITC-dextran (21). For TEER assays, cells were grown on 12-mm gold-coated ECIS grids (8W1E), and real-time impedance was acquired by using a 1600R device and firm software to derive TEERs. Detailed methods are available in *SI Materials and Methods* and Table S1.

In vivo permeability measurements in occluded pial microvessels were performed on rats as described by Hudson et al. (21), and details are provided in *SI Materials and Methods*.

References

1. Klaassen I, Van Noorden CJF, Schlingemann RO (2013) Molecular basis of the inner blood-retinal barrier and its breakdown in diabetic macular edema and other pathological conditions. Prog Retin Eye Res 34:19 – 48.

2. Stitt AW, et al. (2016) The progress in understanding and treatment of diabetic retinopathy. Prog Retin Eye Res 51:156– 186.

3. Brown DM, et al.; RIDE and RISE Research Group (2013) Long-term outcomes of ranibizumab therapy for diabetic macular edema: The 36-month results from two phase III trials: RISE and RIDE. Ophthalmology 120(10):2013–2022.

4. Ford JA, et al. (2013) Current treatments in diabetic macular oedema: Systematic review and meta-analysis. BMJ Open 3(3):e002269.

5. Ciulla TA, Hussain RM, Ciulla LM, Sink B, Harris A (2015) Ranibizumab for diabetic macular edema refractory to multiple prior treatments [published online ahead of print November 18, 2015]. Retina , doi: 10.1097/IAE.0000000000000876.

6. Kurihara T, Westenskow PD, Bravo S, Aguilar E, Friedlander M (2012) Targeted deletion of Vegfa in adult mice induces vision loss. J Clin Invest 122(11):4213 – 4217.

7. Iwase M, et al. (2008) Lysophosphatidylcholine contents in plasma LDL in patients with type 2 diabetes mellitus: Relation with lipoprotein-associated phospholipase A2 and effects of simvastatin treatment. Atherosclerosis 196(2):931–936.

8. Huang F, et al. (2005) Lysophosphatidylcholine increases endothelial permeability: Role ofPKCalpha and RhoA cross talk.Am J Physiol Lung Cell Mol Physiol 289(2):L176–L185.

9. Silva IT, Mello AP, Damasceno NR (2011) Antioxidant and inflammatory aspects of lipoprotein-associated phospholipase A_2(Lp-PLA_2): A review. Lipids Health Dis 10:170.

10. Oei HHS, et al. (2005) Lipoprotein-associated phospholipase A2 activity is associated with risk of coronary heart disease and ischemic stroke: The Rotterdam Study. Circulation 111(5):570–575.

11. Katan M, et al. (2014) Lipoprotein-associated phospholipase A2 is associated with atherosclerotic stroke risk: The Northern Manhattan Study. PLoS One 9(1):e83393.

12. Thompson A, et al.; Lp-PLA(2) Studies Collaboration (2010) Lipoprotein-associated phospholipase A(2) and risk of coronary disease, stroke, and mortality: Collaborative analysis of 32 prospective studies. Lancet 375(9725):1536–1544.

13. Stafforini DM, Elstad MR, McIntyre TM, Zimmerman GA, Prescott SM (1990) Human macrophages secret platelet-activating factor acetylhydrolase.J Biol Chem 265(17): 9682–9687.

14. Doublier S, et al. (2007) The proangiogenic phenotype of tumor-derived endothelial cells is reverted by the overexpression of platelet-activating factor acetylhydrolase. Clin Cancer Res 13(19):5710–5718.

15. Wilensky RL, et al. (2008) Inhibition of lipoprotein-associated phospholipase A2 reduces complex coronary atherosclerotic plaque development. Nat Med 14(10):1059 –1066.

16. Wang WY, et al. (2011) Inhibition of lipoprotein-associated phospholipase A2 ameliorates inflammation and decreases atherosclerotic plaque formation in ApoE-deficient mice. PLoS One 6(8):e23425.

17. Acharya NK, et al. (2013) Diabetes and hypercholesterolemia increase blood-brain barrier permeability and brain amyloid deposition: Beneficial effects of the LpPLA2 inhibitor darapladib. J Alzheimers Dis 35(1):179–198.

18. Roberts A (2014) Coronary artery disease: Darapladib fails to improve the STABILITYof CAD. Nat Rev Cardiol 11(6):310.

19. Staurenghi G, et al. (2015) Darapladib, a lipoprotein-associated phospholipase A inhibitor,in diabetic macular edema: A 3-month placebo-controlled study. Ophthalmology 122(5):990–996.

20. Zhang SX, et al. (2005) Genetic difference in susceptibility to the blood-retina barrier breakdown in diabetes and oxygen-induced retinopathy. Am J Pathol 166(1):313–321.

21. Hudson N, et al. (2014) Differential apicobasal VEGF signaling at vascular blood-neural barriers. Dev Cell 30(5):541–552.

22. Wilensky RL, Macphee CH (2009) Lipoprotein-associated phospholipase A(2) and atherosclerosis. Curr Opin Lipidol 20(5):415–420.

23. Wu M, et al. (2008) Intraretinal leakage and oxidation of LDL in diabetic retinopathy. Invest Ophthalmol Vis Sci 49(6):2679–2685.

24. Lavi S, et al. (2007) Local production of lipoprotein-associated phospholipase A2 and lysophosphatidylcholine in the coronary circulation: Association with early coronary atherosclerosis and endothelial dysfunction in humans. Circulation 115(21):2715–2721.

25. Qaum T, et al. (2001) VEGF-initiated blood-retinal barrier breakdown in early diabetes. Invest Ophthalmol Vis Sci 42(10):2408–413.

26. Chen X, et al. (2016) Discovery of potent and orally active lipoprotein-associated phospholipase A2 (Lp-PLA2) inhibitors as a potential therapy for diabetic macular edema. J Med Chem 59(6):2674–2687.

27. Carneiro AB, et al. (2013) Lysophosphatidylcholine triggers TLR2- and TLR4-mediated signaling pathways but counteracts LPS-induced NO synthesis in peritoneal macrophages by inhibiting NF-κB translocation and MAPK/ERK phosphorylation.PLoS One 8(9):e76233.

28. Schaeffer DF, et al. (2009) LOX-1 augments oxLDL uptake by lysoPC-stimulated murine macrophages but is not required for oxLDL clearance from plasma. J Lipid Res 50(8):1676–1684.

29. Vladykovskaya E, et al. (2011) Reductive metabolism increases the proinflammatory activity of aldehyde phospholipids. J Lipid Res 52(12):2209–2225.

30. Qiao J, et al. (2006) Lysophosphatidylcholine impairs endothelial barrier function through the G protein-coupled receptor GPR4. Am J Physiol Lung Cell Mol Physiol 291(1):L91–L101.

31. Fujita Y, et al. (2006) Transactivation of fetal liver kinase-1/kinase-insert domain-containing receptor by lysophosphatidylcholine induces vascular endothelial cell proliferation. Endocrinology 147(3):1377–1385.

32. Warren CM, Ziyad S, Briot A, Der A, Iruel a-Arispe ML (2014) A ligand-independent VEGFR2 signaling pathway limits angiogenic responses in diabetes. Sci Signal 7(307):ra1.

33. Barber AJ, Antonetti DA, Gardner TW; The Penn State Retina Research Group (2000) Altered expression of retinal occludin and glial fibrillary acidic protein in experimental diabetes. Invest Ophthalmol Vis Sci 41 (11): 3561– 3568.

34. Hofman P, et al. (2000) VEGF-A induced hyperpermeability of blood-retinal barrier endothelium in vivo is predominantly associated with pinocytotic vesicular transport and not with formation of fenestrations. Vascular endothelial growth factor-A. Curr Eye Res 21(2):637–645.

35. Schmidt-Erfurth U, et al.; RESTORE Extension Study Group (2014) Three-year outcomes of individualized ranibizumab treatment in patients with diabetic macular edema: The RESTORE extension study. Ophthalmology 121(5):1045–1053.

36. Blackie JA, et al. (2003) The identification of clinical candidate SB-480848: A potent inhibitor of lipoprotein-associated phospholipase A2. Bioorg Med Chem Lett 13(6):1067–1070.

37. Blackie JA, et al. (2002) The discovery of SB-435495. A potent, orally active inhibitor of lipoprotein-associated phospholipase A(2) for evaluation in man. Bioorg Med Chem Lett 12(18):2603–2606.

38. Crawford GL, et al. (2015) The role of lipoprotein-associated phospholipase A2 in a murine model of experimental autoimmune uveoretinitis. PLoS One 10(4):e0122093.

39. Greenwood J, et al. (1996) SV40 large T immortalised cell lines of the rat blood-brain and blood-retinal barriers retain their phenotypic and immunological characteristics. J Neuroimmunol 71(1-2):51–63.

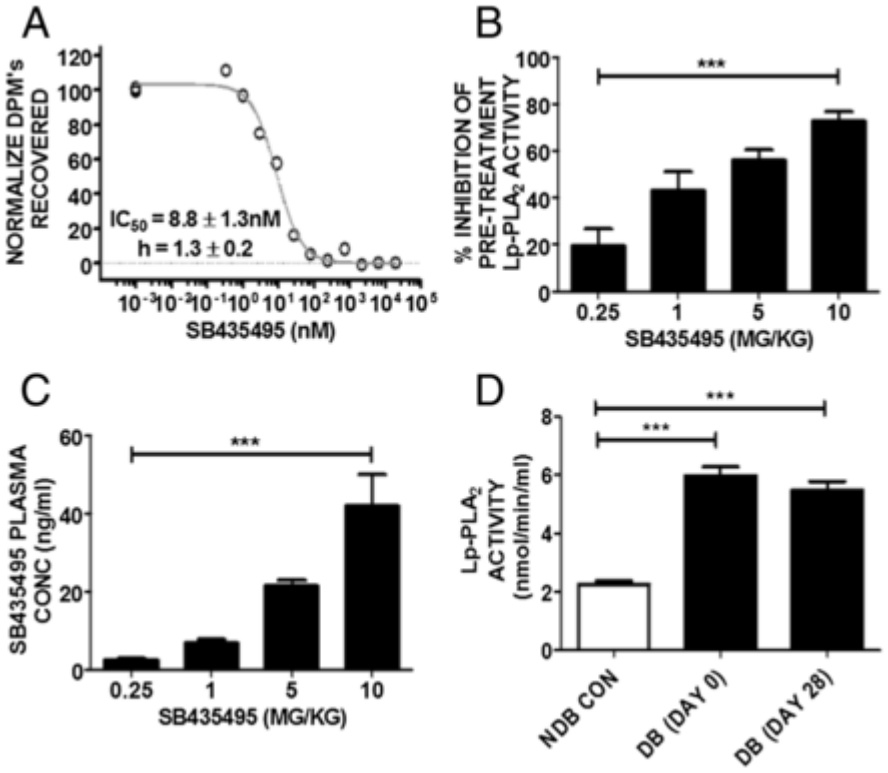

Fig. 1. Lp-PLA_2 inhibition and SB435495 plasma concentration in BN rat plasma. (*A*) Lp-PLA_2 activity was measured in the presence of increasing concentrations of SB435495. The IC_{50} was calculated as 8.8 ± 1.3 nM. (*B*) Activity of Lp-PLA_2 was measured following SB435495 administration for 28 d in diabetic rats. Mean ± SEM are shown, $n = 8$ per treatment group (***$P = 0.0001$, one-way ANOVA analysis). (*C*) Mean systemic SB435495 concentrations in terminal plasma samples from BN rats. SB435495 concentrations were detected by HPLC/MS/MS expressed in ng/mL (***$P < 0.0001$, one-way ANOVA analysis) ($n = 12$ for 10, 5, and 1 mg/kg groups, $n = 11$ for 0.25 mg/kg SB435495 group). (*D*) Lp-PLA_2 activity in diabetic (DB) and nondiabetic (NDB) rat plasma collected at day 0 and day 28 of diabetes. Diabetes significantly increased Lp-PLA_2 activity ($P < 0.0001$), which was sustained throughout the duration of the experiment. $n = 13$ NDB CON, $n = 10$ DB (day 0), $n = 12$ DB (day 28).

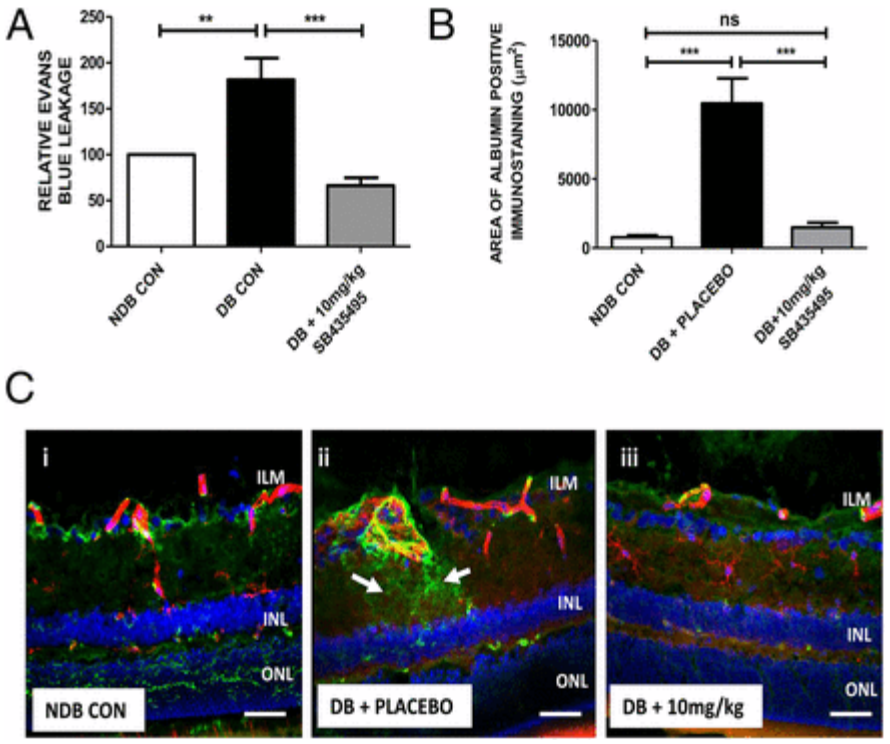

Fig. 2. Suppression of diabetes-induced retinal vasopermeability by SB435495. (*A*) Quantification of Evans blue leakage into the retina was measured in nondiabetic (NDB) control, diabetic controls (DB CON), or SB435495-treated diabetic rats. Retinal vasopermeability was significantly increased in DB CON compared with NDB (**P = 0.047, $P < 0.05$, t test). Lp-PLA_2 inhibition with 10 mg/kg SB435495 reduced BRB breakdown (***P = 0.002, t test). Mean ± SEM, n = at least 8 animals per group. (*B*) Mean area of albumin-positive immunostaining in square micrometers measured in retinal sections dual stained with isolectin B4 and anti-rat albumin antibody. There was a statistically significant increase in albumin immunoreactivity in the DB CON sections, compared with NDB sections (***$P < 0.0001$, Mann–Whitney test). SB435495 (10 mg/kg) treatment reduced albumin immunoreactivity to that observed in the NDB retinal sections (***$P < 0.0001$, Mann–Whitney test). Means ± SEM n = 3 animals per group, 16 images per treatment analyzed. (*C*) Representative images of albumin/isolecin B4-stained retinal sections from NDB, DB CON, and SB435495-treated rats. Red channel, isolectin B4; green channel, anti-rat albumin; blue channel, DAPI. Significant vascular leak was observed in the diabetic + placebo-treated animals (*ii*) compared with nondiabetic controls (*i*). Albumin leakage was reduced in the 10 mg/kg SB435495 group (*iii*). (Objective magnification: 40×.) n = 3 animals per treatment group. (Scale bars: 50 µm.)

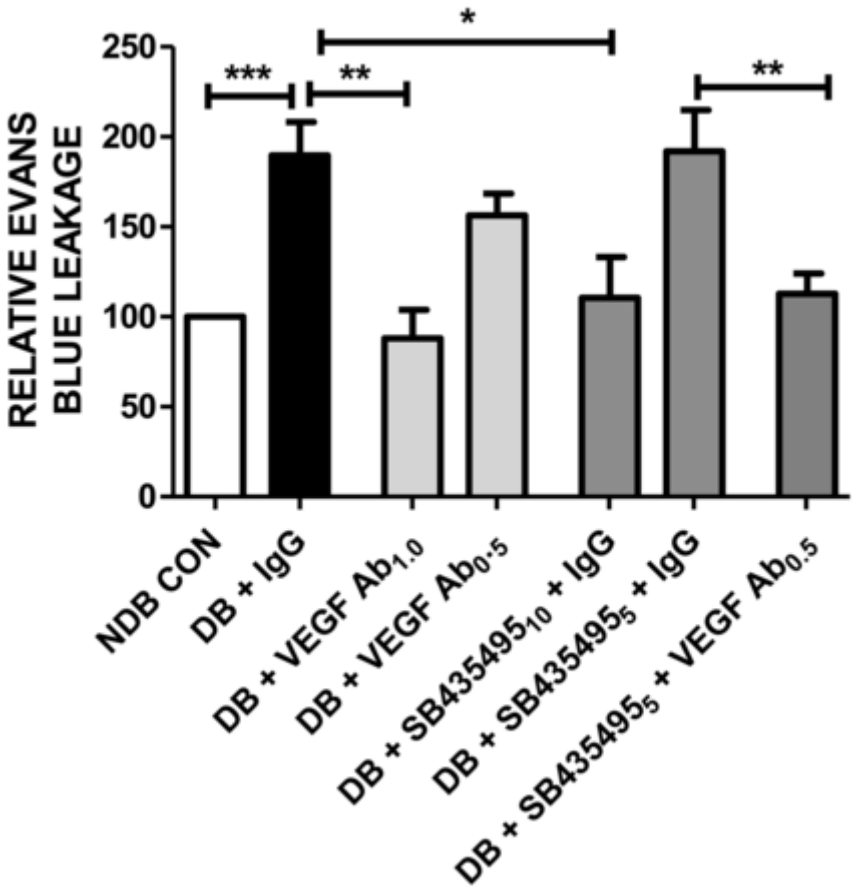

Fig. 3. Inhibition of retinal vasopermeability by Lp-PLA_2. Effect of combined SB435495 and intravitreal DMS1529 (anti-VEGF domain antibody) on retinal vasopermeability in diabetic (DB) rats. SB435495 was given i.p. daily at the indicated doses. VEGF antibody (DMS1529) or isotype-matched IgG were bilaterally injected intravitreally at day 26. Retinal vasopermeability was significantly elevated in DB + IgG-treated rats, compared with NDB controls (one-way ANOVA, Bonferroni post test ***$P < 0.05$) (Fig. 3). Treatment with 1.0 mg/mL anti-VEGF antibody or 10 mg/kg SB435495 +IgG treatment resulted in a significant reduction in retinal leakage compared with DB + IgG-treated rats (one-way ANOVA, Bonferroni post hoc test ***$P < 0.05$). Treatment with 0.5 mg/mL anti-VEGF antibody alone or suboptimal 5 mg/kg SB435495 + IgG treatment had no effect on retinal vasopermeability. However, 0.5 mg/mL anti-VEGF antibody + 5 mg/kg SB435495 (suboptimal dose) treatment induced a significant reduction in retinal vasopermeability, compared with DB animals treated with 5 mg/kg SB435495 + IgG (one-way ANOVA, Bonferroni post hoc test **$P < 0.05$). Mean ± SEM, n = at least 14 animals per treatment group. 10 and 5, 10 and 5 mg/kg SB435495; 1.0 and 0.5, 1.0 and 0.5 mg/mL DMS1529 or IgG.

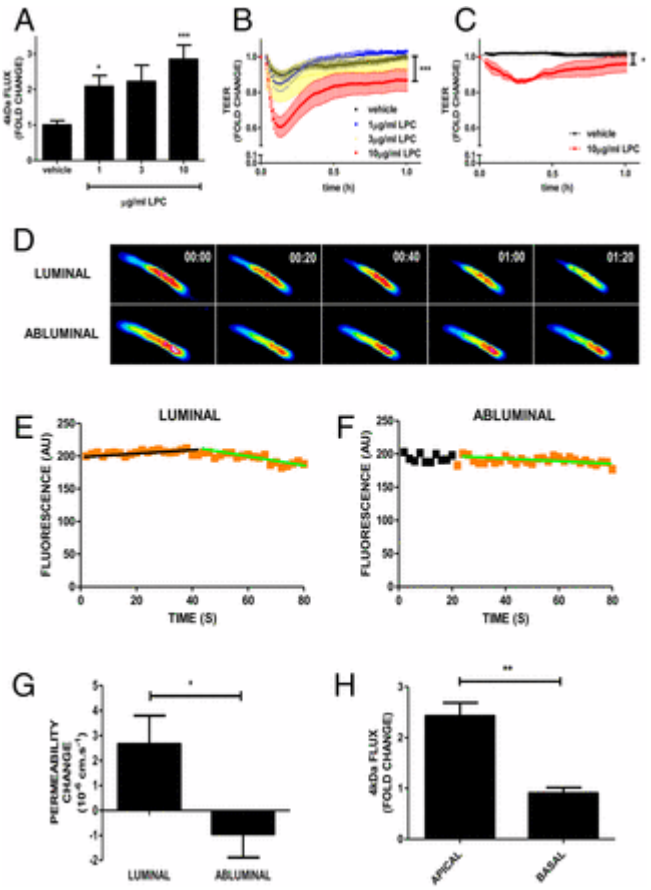

Fig. 4. Effects of increased concentration of LPC on neural MVEC barriers. (*A*) Four-kilodalton dextran flux was measured in primary brain MVECs before and after the addition of the indicated concentrations of LPC. Shown are means ± SEM (n = 8 for vehicle, n = 4 for 1 μg/mL LPC, n = 5 for 3 μg/mL LPC, n = 10 for 10 μg/mL LPC) of averaged 2-h flux [one-way ANOVA (P = 0.022) Bonferroni post hoc tests: *P < 0.05, **P < 0.01]. (*B* and *C*) Primary rat brain (*B*) and retinal (*C*) EC were grown to confluence and until they reached full electrical barrier (TEER of approximately 25,000 Ω and 15,000 Ω, respectively). LPC was added at the indicated concentrations at time 0. Shown are means (± SEM) of normalized resistance changes. There were differences for both brain and retinal MVECs (brain MVECs: P < 0.0001) (retinal MVECs: P < 0.004) with Bonferroni post hoc analysis, indicating significant differences between vehicle and 10 μg/mL LPC (brain: P < 0.0001; retina: P < 0.05). (*D*) LPC induces microvascular permeability in pial vessels in vivo. Time-dependent recording of sulforhodamine B (580 Da) loss from single occluded rat pial microvessels in vivo. Luminal injection (via intracarotid) of 30 μg/mL LPC (assumed diluted to 10–15 μg/mL final in the brain) produced a strong decrease of sulforhodamine B after approximately 40 s. Abluminal application of LPC (10 μg/mL) through a cranial window at t = 20 s did not lead to any changes in permeability. Micrographs of pseudocolored microvessels at indicated times (minutes). Mean densitometric fluorescent intensities in microvessels plotted against time (*E* and *F*). Data were fitted (black and green trend lines) to the equation $C_t = C_0 \cdot e^{-kt}$. Black and orange data points represent times without and with LPC, respectively. (*G*) Mean permeability changes acquired as shown in *D* following abluminal (10 μg/mL; n = 4) and luminal LPC (assumed 10–15 μg/mL final; n = 8) ± SEM P < 0.05 (Student's t test). (*H*) Primary brain MVECs were grown on Transwell filters, and the flux of 4-kDa dextran was measured in response to apically or basally added LPC (10 μg/mL). Shown are means ± SEM (P < 0.01, Student's t test).

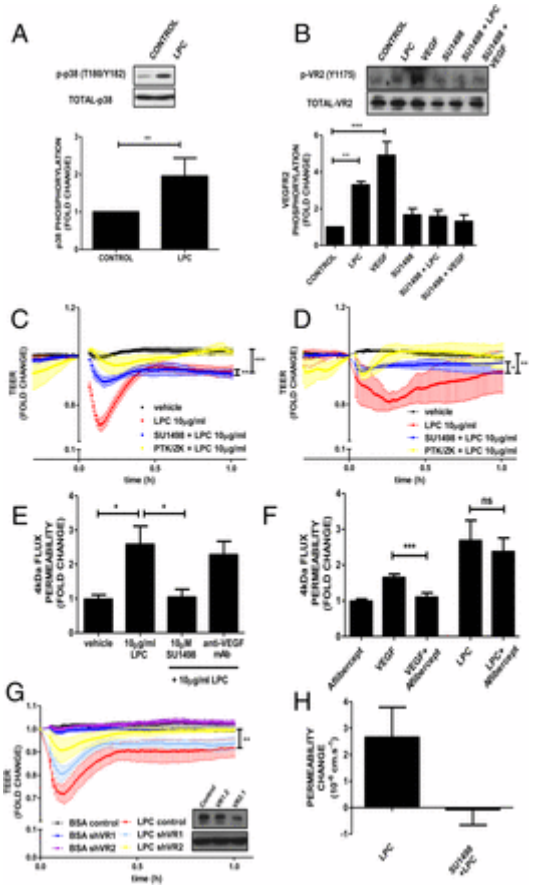

Fig. 5. Leakage induction of LPC via VEGFR2 signaling pathway. (*A*) Rat retinal MVECs (PT2) treated with LPC (10 μg/mL), and levels of phosphorylated p38 (pT180/Y182) were determined by Western blotting. Shown is a representative blot and normalized densitometric quantifications (means ± SEM, $n = 3$, $^{**}P < 0.01$, Student's *t* test). (*B*) As in *A*, except that PT2 were pretreated with SU1498 (10 μM) for 1 h where indicated and then with LPC (10 μg/mL) or VEGF-A (50 ng/mL) for 5 min, and samples were immunoblotted for both phosphorylated (Y1175) and total VEGFR2. Shown are means ± SEM ($n = 3$) from one-way ANOVA analysis ($P < 0.0001$) (Dunnett's post hoc test showed significant differences for LPC and VEGF ($P < 0.01$ and $P < 0.0001$, respectively). (*C*) Primary rat brain EC were grown to confluence and until they reached full electrical barrier. At times, 1-h cells were pretreated or not with SU1498 or PTK/ZK (both at 10 μM). LPC was added at time 0. Shown are means of normalized resistance changes. (*D*) Primary rat MVECs were grown to confluence and until they reached full electrical barrier and treated/analyzed as in *C*. One-way ANOVA ($P < 0.01$), Bonferroni post hoc test show significant differences between vehicle vs. LPC ($P < 0.01$) and LPC vs. LPC+PTK ($P < 0.01$) and LPC vs. LPC+SU ($P < 0.05$) (*E*) Postconfluent primary MVECs were pretreated in the presence or absence of SU1498 (10 μM) or DMS1529 (10 μg/mL) and 4-kDa dextran flux was measured before and after the addition of 10 μg/mL LPC. Means ± SEM (vehicle, $n = 8$; LPC, $n = 8$; SU+LPC, $n = 8$; DMS+LPC, $n = 4$) for one-way ANOVA and Dunnett's post hoc test: $^{*}P < 0.05$. (*F*) Flux experiment as described in *E* except that aflibercept (EYLEA**;** 25 μg/mL) was added or not before measuring the flux induced by VEGF-A (50 ng/mL) or LPC (10 μg/mL). Significant increases in flux induced by VEGF-A were reversed by Aflibercept ($^{***}P < 0.01$; Student's *t* test). However, aflibercept did not reverse flux increases induced by LPC (not significant, Student's *t* test). (*G*) Primary rat brain MVEC were grown until confluence and until they reached full electrical barrier and infected with shRNA-encoding adenovirus at a multiplicity of infection (m.o.i.) of 400, targeting either VEGFR1 (shVR1.2) or VEGFR2 (shVR2.1). Forty-eight hours after infection, LPC (10 μg/mL) was added (time 0). Corresponding protein knockdown is shown in *Inset*. One-way ANOVA ($P < 0.0001$), Bonferroni post hoc analysis showed significant differences between BSA vs. LPC ($P < 0.001$) and LPC vs. VR2.1+LPC ($P < 0.01$) but not LPC vs. VR1.2+LPC ($n = 4$). (*H*) Permeability in pial rat microvessels in vivo following 20 μM SU1498 pretreatment for 15 min before sulforhodamine loss in response to luminal LPC (10–15 μg/mL final) from occluded pial microvessels. Shown are mean (± SEM). $^{*}P < 0.05$ (Student's *t* test).

SI Materials and Methods

Lp-PLA$_2$ Inhibition in Diabetic Rats.

Diabetes was induced in male adult BN rats (150–190 g) by a single i.p. injection of streptozotocin (STZ; Sigma Aldrich) (60–65 mg/kg in 0.1 mol/L citrate buffer, pH 4.6). Diabetes in these animals is accompanied by sustained compromise of the BRB (20). At 10 d after STZ injection, glucometric analysis of tail prick blood samples (Breeze2; Bayer) was used to select diabetic animals (hyperglycemic with blood glucose concentration >15 mmol/L) for the remainder of the study. HbA_{1c} (glycated hemoglobin) levels were measured in terminal blood samples by using Glyco-Tek Affinity Columns (Helena Biosciences Europe).

SB-435495 and SB-568859 (GlaxoSmithKline) are potent and selective pharmacological inhibitors of Lp-PLA$_2$ in a variety of species (36, 37). Pharmacokinetic analysis in a number of species suggested that the pharmacokinetic properties of SB-568859 were most applicable to studies in rabbits, whereas the properties of SB-435495 were best suited for studies in rat (38). SB435495 was formulated as a solution in 10% Captisol (Hovione) with 10 mM sodium acetate pH 4.5. For assessment of Lp-PLA$_2$ inhibition by SB435495, blood samples were collected 24 h before treatment and 24 h after the final placebo/SB435495 drug dosing. Plasma was prepared by centrifugation at 13,000 × *g* and stored at −80 °C. SB435495 concentration was measured in 25-μL plasma samples by using an analytical method based on protein precipitation, followed by HPLC/MS/MS analysis (detection range 1 ng/mL to 1,000 ng/mL). Lp-PLA$_2$ activity was evaluated by determining the enzyme-catalyzed release of [^{3}H-] acetate from 1-*O*-Hexadecyl-2-*O*-[^{3}H-]acetyl-sn-glycer-3-phophorylcholine. Reactions were extracted by using chloroform:methanol (1:1) and disintegrations per unit time (DPMs) in the aqueous layer determined by liquid scintillation counting. DPMs were converted to moles of product through normalization to a [^{3}H-] PAF standard.

Effects of Lp-PLA$_2$ Inhibition of Diabetes-Induced Retinal Vasopermeability.

BN rats were confirmed diabetic 10 d after STZ treatment and then randomly assigned into groups receiving either a once-daily i.p. injection of placebo (vehicle) or once-daily dosing of SB435495 (dosing at 10 mg/kg, 5 mg/kg, 1 mg/kg, and 0.25 mg/kg). A separate group of nondiabetic, age-matched control BN rats received no treatment. After 28 d, animals were processed for analysis of retinal vascular leakage. In additional studies where the effect of combination of anti-VEGF and SB435495 therapies on diabetes-induced retinal vasopermeability was studied, anti-VEGF or control antibodies were introduced by intravitreal injections (1 μL volume) in both eyes, at day 26 after initial SB435495 administration.

Retinal vasopermeability indicating breakdown of the BRB was assessed by using the Evans blue assay as described. Briefly, Evans blue dye (30 mg/mL in PBS) (Sigma Aldrich) was administered through the tail vein (45 mg/kg) and allowed to circulate for 2 h before animals were terminally anesthetized with sodium pentobarbital. An intracardiac blood sample was collected before perfusion (20 mL/min for 5 min) through the left ventricle with 0.1 M citrate buffer pH 3.5. Retinas were isolated, freeze-dried, and extracted with formamide. Evans blue recovery in clarified samples was determined spectrophotometrically at 620 nm and 740 nm and compared with terminal plasma samples collected from the same animals. Concentrations of Evans blue were derived from standard curves of the dye in formamide.

Rat Retinal Immunostaining.

Enucleated eyes were fixed in 4% paraformaldehyde. Eyes were bisected at the equator, cryoprotected by sequential overnight immersion in 10%, 20%, and 30% sucrose solution, and then embedded in optimal cutting temperature medium (CellPath Ltd). Serial 20-μm cryosections from the central and opposing peripheral retinal regions were collected on Superfrost plus slides. Frozen sections were rehydrated in 3% Triton X-100 in TBS for 30 min and blocked for 1 h in 1% donkey serum. Sections were incubated overnight at 4 °C with sheep anti-rat albumin antibody (1:500 dilution) (Bethyl Laboratories) and biotinylated *Griffonia simplicifolia* isolectin B4 (20 μg/mL) in blocking buffer (Sigma Aldrich). Sections were washed and stained with donkey anti-sheep Alexa Fluor 488 nm and streptavidin Alexa Fluor 568 nm. Sections were counterstained with DAPI, mounted with Vectashield (Vector Labs), and images captured with a confocal scanning laser microscope (Eclipse

TE2000-U confocal microscope, Nikon). The area of albumin immunoreactivity in captured images was quantified by using Nikon NIS Elements image analysis software.

Effects of Lp-PLA$_2$ Inhibition on VEGF-Induced Retinal Vascular Hyperpermeability in Rabbits.

Male HY79b pigmented rabbits (1,800–2,200 g, Hypharm) were treated with SB568859 (GlaxoSmithKline), a potent rabbit Lp-PLA$_2$ inhibitor. SB568859 was administered orally, at 0 (vehicle alone), 3, 10, and 30 mg/kg, respectively, once on day 1, twice (8:00 AM and 4:00 PM) on days 2–5, and once on day 6. As positive control, 2-mg triamcinolone acetonide (Kenacort) was injected into the vitreous on day 1. Retinal vascular leakage was induced through the intravitreal injection of 500 ng of recombinant VEGF (rhVEGF; R&D Systems) in the right eye of all animals on day 4. Blood samples were collected on day 4 and day 5 (before the scheduled SB568859 dosing, equivalent to C_{trough}), and on day 6 (~2–3 h after the day 6 SB568859 dosing) for determination of SB568859 concentration and Lp-PLA$_2$ enzyme activity. Fluorescein angiography and ocular fluorophotometry (FM) measurements were performed on day 6 to assess retinal vascular permeability. Forty-seven hours after rhVEGF injection, and 1 h (± 15 min) after the last SB568859 dosing, sodium fluorescein (10% in saline solution 0.9%, 50 mg/kg) was injected into anesthetized rabbits via the marginal ear vein. After injection of the fluorescein tracer, three retinal angiograms (corresponding to the nasal, central and temporal retina) of the right eye were recorded by using a Heidelberg Retinal Angiograph (HRA, Heidelberg Engineering). All angiography images were assessed for retinal leakage by masked scoring by three individuals, using the following scoring system: 0, no leakage; 1, slight leakage; 2, moderate leakage; and 3, severe leakage. Leakage values were then averaged to assess changes in the BRB breakdown. In addition, 1 h following fluorescein injection, the presence of fluorophore was recorded in both eyes with a FM-2 Fluorotron Master ocular fluorophotometer (OcuMetrics). A series of 148 scans with a 0.25-mm step size were recorded from the cornea to the retina along the optical axis. The ratio of fluorescein content between the vitroretinal compartment of the right and left eyes was used to evaluate changes to the BRB.

MVECs.

Primary MVECs were isolated from rat brains or retinae and grown as described (21). Briefly, microvessels were isolated by enzymatic and mechanical disruption of tissue, purified on BSA and Percoll gradients, and further selected for by treatment with puromycin. Cells were seeded onto collagen IV/fibronectin and grown in EGM2-MV media (Lonza). A stable rat retinal MVEC line (PT2) was also used to provide the larger cell quantities necessary for biochemical analyses. These cells were derived from primary rat retinal MVECs by immortalization with a temperature-sensitive (tsa58) SV40 large T encoding retrovirus (39) and subsequent cloning. PT2s were grown on collagen IV/fibronectin in EGM2-MV media (Lonza).

Recombinant Adenoviruses.

Double-stranded oligonucleotides designed to encode small hairpin RNAs targeting either mouse and rat VEGFR1 (GATCCCGCCACATCGGCCATCATCTGAAGGAATTCGTTCAGATGATGGCCGATGTGGTTTTTA) or VEGFR2 (GATCCCGCCATGTTCTTCTGGCTCCTTCGGAATTCGGAAGGAGCCAGAAGAACATGGTTTTTA) were subcloned into BamH1/Hind3 sites of pRNAT-H1.1/Shuttle (GenScript), where the transcript in question and that of GFP are under the control of the H1.1 and CMV promoter, respectively. Effectiveness of knockdown by these constructs was confirmed by transient transfection in the MVEC cell line. Subsequently, recombinant adenoviruses were prepared from these shuttle plasmids (VectorBiolabs). High-titer viral stocks were kept at −80 °C and used to infect primary MVECs at m.o.i. of 50–2,000.

Vascular Permeability in Retinal and Brain MVECs.

LPC (Cayman Chemical Company) was diluted into PBS, which was supplemented with 0.1% fatty-acid free BSA. SU1498 (Sigma) and PTK787/ZK222584 (PTK/ZK) were diluted from freshly made stocks (10 mM in DMSO). Flux measurements were performed as described by using 4-kDa FITC dextran (21). Briefly, cells were grown on transwells (6.5 mm, 0.4-μm pores; Corning) and dextran (1 mg/mL) added to the apical side. Flux was monitored in samples (30 μL) taken from the basal side at 20- to 30-min intervals. Baseline flux was recorded from untreated cells for 120 min, followed (optionally) by the baseline in the presence of small

molecule inhibitors for at least another 60 min, and finally for an additional 120 min from when the vasoactive compounds were added. Fluorescence of samples was plotted against time and permeability changes were determined from linear slope changes average over 2 h before and after addition of the compound. LPC (10 μg/mL) was added apically or basally for directionality experiments. Postconfluent primary MVECs were pretreated in the presence or absence of SU1498 (10 μM) or DMS1529 (10 μg/mL), and 4-kDa dextran flux was measured before and after the addition of 10 μg/mL LPC. In additional flux studies aflibercept (EYLEA; 25 μg/mL) was added or not before measuring the flux induced by VEGF-A (50 ng/mL) or LPC (10 μg/mL).

For TEER assays, cells were grown on 12-mm gold-coated ECIS grids (8W1E) and real-time impedance was acquired by using a 1600R device and firm software (all Applied Biophysics) to derive TEERs. At the start of experiments, TEER values were approximately 25,000 Ω and 15,000 Ω for brain and retinal MVECs, respectively.

Vascular Permeability in Pial Microvessels in Vivo.

In vivo permeability measurements in occluded pial microvessels were performed on Wistar rats (aged 25–30 d) exactly as described by Hudson et al. (21). Briefly, the vasculature was filled with sulforhodamine B (580 Da, Sigma) before a microvessel on the pial surface was occluded by using a glass probe. Time-dependent loss of fluorescent signal from the occluded microvessels is solely due to permeability and was recorded by using video microscopy. Intensity mapping then allows calculation of vessel permeability and time-dependent changes using $C_t = C_0 \cdot e^{-kt}$; where $k = 4P/d$, and where C_t and C_0 are the dye concentrations at time t and time 0, respectively; P is the permeability and d the diameter of the vessel. LPC was either delivered through the carotid artery (luminal application) or applied to a cranial window (abluminal) at various concentrations. Antagonist pretreatment was via the cranial window for 15 min before LPC application and permeability measurements.

Immunoblot Analysis.

For immunoblot analyses, treated PT2 cells were lysed in 50 mM Tris/Cl, pH 6.8, 2% SDS, 10% glycerol, 100 mM DTT, (50 μL/cm^2 of cells), separated by SDS/PAGE and electrotransfered to nitrocellulose or PVDF. For each series of samples, two identically loaded gels/immunoblots were run for immunodecoration with phospho-specific and total antibodies. All primary antibodies were from Cell Signaling Technology: anti-phospho-VEGFR2 (Y1175), anti-VEGFR2 (55B11), anti-phospho-p38 (T180/Y182) (9211), and anti-p38 (9212).

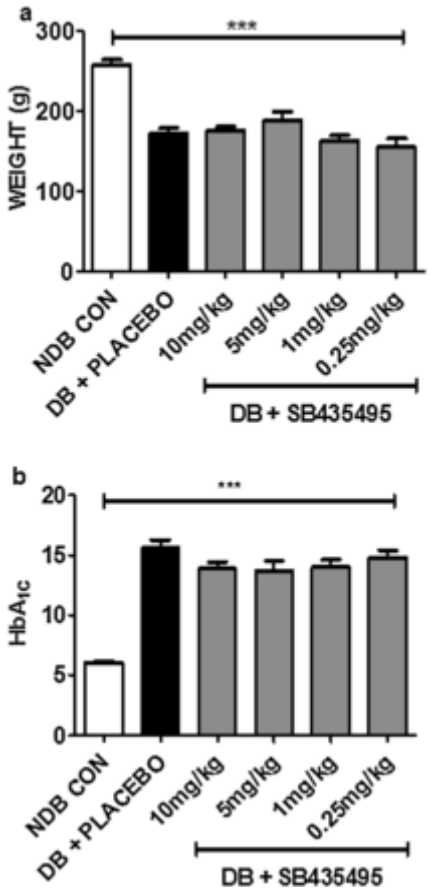

Fig. S1. Characterization of BN rats following induction of diabetes and 28-d dosing with the selective Lp-PLA_2 inhibitor SB435495. (*A*) Mean change in rat body weight over the course of the experiment. Diabetic (DB) animals gained significantly less body weight over the course of the experiment compared with the nondiabetic (NDB) control group of animals. One-way ANOVA (***$P < 0.001$). (*B*) Associated HbA_{1c} levels in BN rats, 28 d after initial SB435495 dosing. Placebo-treated and SB435495-treated DB rats had significantly elevated glycated hemoglobin levels compared with NDB control animals, and drug-treatment had no effect on overall HbA_{1c} levels. One-way ANOVA (***$P < 0.001$).

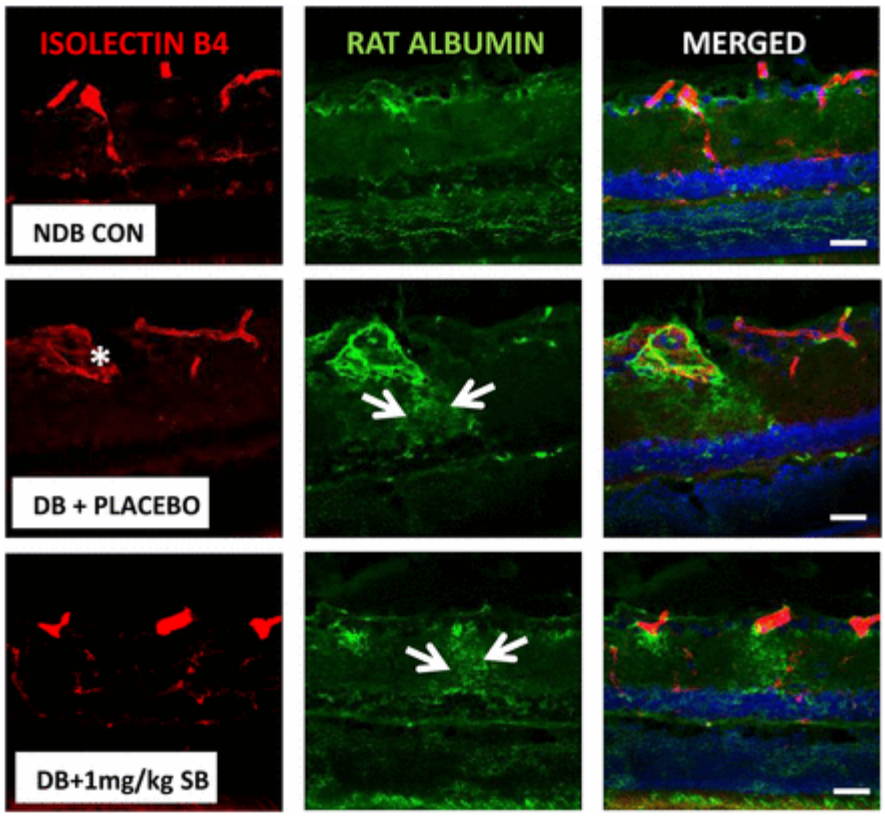

Fig. S2. Histological assessment of diabetes-induced retinal vasopermeability in BN rats. Representative rat retinal sections stained with isolectin B4 to assess retinal vasculature (red), and anti-rat albumin antibody (green) to assess albumin extravsation from the retinal vessels. Significant vascular leakage of albumin was observed in the diabetic (DB) placebo-treated animals compared with nondiabetic (NDB) control animals. This leakage, indicated by the arrows on the micrographs, primarily emanated from dilated retinal vessels (marked with an asterisk) and was focal in nature. Low-dose (1 mg/kg) SB435495 treatment resulted in the reestablishment of areas of retinal vasopermeability, which also arose from dilated vessels. (Objective magnification: 40×.) (Scale bars: 50 µm.)

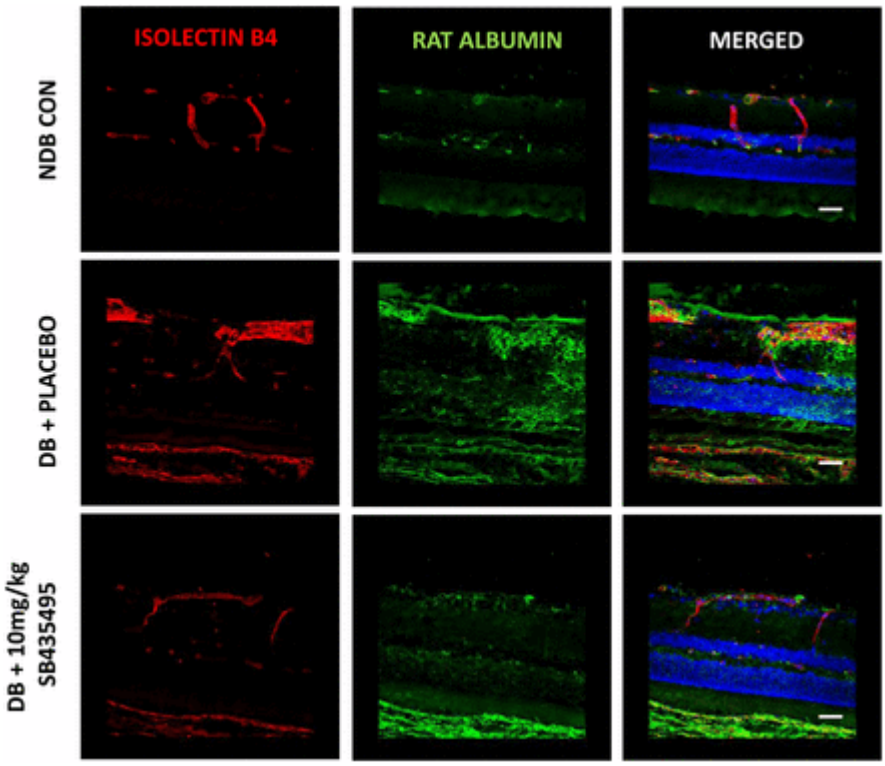

Fig. S3. Efficacy of SB435495 administered curatively to prevent diabetes-induced albumin extravasation. BN rats were rendered diabetic by a single i.p. injection of STZ and maintained hyperglycemic for 28 d before receiving a single daily i.p. injection of placebo or 10 mg/kg SB435495 for a further 28 d. At the end of the experimental period, retinal vascular permeability was assessed by confocal microscopy of rat retinal sections for extravasted albumin. Significant vascular leak was observed in the diabetic (DB) placebo-treated animals compared with the nondiabetic (NDB) control animals. Albumin leakage was markedly less pronounced in the 10 mg/kg SB435495-treated rats. *n* = 3 animals per treatment group. (Objective magnification: 40×.) (Scale bars: 50 µm.)

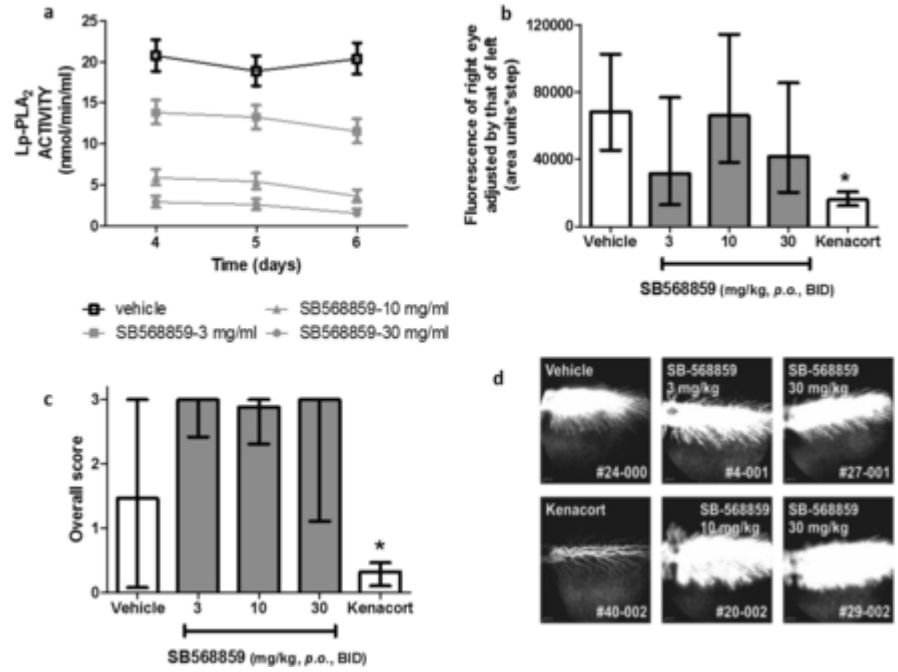

Fig. S4. Effect of Lp-PLA_2 inhibition in VEGF-induced retinal leak in HY79b-pigmented rabbits. HY79b-pigmented male rabbits were treated with SB568859 at 0 (vehicle alone) (*n* = 6), 3 (*n* = 6), 10 (*n* = 8), and 30 mg/kg, respectively (*n* = 8), once on day 1, twice (8:00 AM and 4:00 PM) on days 2–5, and once on day 6. On day 4, 500 ng of rhVEGF was injected intravitreally into the right eye. Retinal vascular leak in the rabbit retina was determined by using fundus fluorescein angiography at day 6. (*A*) Pharmokinetic profile of SB568859 in rabbit plasma at days 4, 5, and 6 following dosing. (*B*) Mean retinal vascular leak in the rabbit retina using flurotron values. Error bars represent 95% confidence limits. One-way ANOVA (**P* < 0.05). (*C*) Retinal vascular leak in the rabbit retina following SB568859 treatment as assessed by morphometric scoring of fluorescein angiography images. Bars represent medians with the 25 and 75 percentiles shown by whiskers. One-way ANOVA, Tukey post test (**P* < 0.05). LPC-induced permeability and VEGF receptor signaling. (*D*) Representative rabbit retinal fluorescein angiograms that were assessed for inhibition of VEGF-induced retinal leakage.

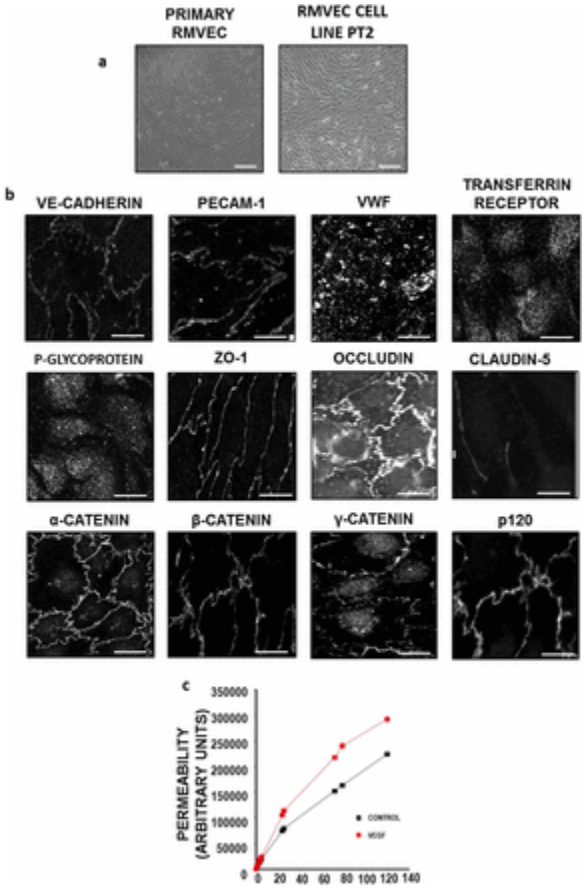

Fig. S5. Characterization of retinal MVECs (PT2). Freshly isolated primary retinal MVECs were immortalized by using a retrovirus coding for temperature-sensitive large T. Immortalized cells were cloned, and one clone termed PT2 was further characterized. PT2 have been maintained for up to 20 passages. TEER was 33.6 (± 7) $\Omega.cm^2$ (*n* = 12) compared with approximately 150 $\Omega.cm^2$ usually achieved in primary retinal MVECs. The permeability coefficient for 4-kDa FITC-dextran flux across PT2 was 21.5 ± 10^{-6} cm/s, *n* = 6) (in parallel experiments, primary brain MVECs gave 3.9 ± 0.6 10^{-6} cm/s, *n* = 5). (*A*) Phase contrast image of confluent primary rat retinal and PT2 MVECs. (*B*) PT2 were stained for fixed and stained for endothelial cell markers: VE-Cadherin, PECAM-1, and von Willebrand Factor (vWF); blood–brain barrier markers: transferrin receptor and p-glycoprotein; and also junctional markers: ZO-1, occludin, claudin-5, α-catenin, β-catenin, γ-catenin, and p120. (*C*) PT2 were grown on permeable transwell supports, and 40-kDa dextran flux was measured in the presence or absence of VEGF (50 ng/mL). (Scale bars: *A*, 50 μm; *B*, 10 μm.)

Group (n = 6–8)	Day 4		Day 5		Day 6	
	PK, ng/mL*	Lp-PLA_2 activity†	PK, ng/mL*	Lp-PLA_2 activity†	PK, ng/mL*	Lp-PLA_2 activity†
Vehicle PO BID‡	BLQ	20.78 ± 0.57	BLQ	18.90 ± 0.43	BLQ	20.40 ± 0.72
SB568859 3 mg/kg PO BID	31.21 ± 3.84	13.95 ± 0.95	27.85 ± 1.71	13.28 ± 0.46	34.87 ± 3.62	12.24 ± 1.33‡
SB568859 10 mg/kg PO BID	48.93 ± 1.88	6.01 ± 0.62	47.76 ± 3.32	5.61 ± 0.39‡	47.55 ± 2.25	3.71 ± 0.41
SB568859 30 mg/kg PO BID	69.79 ± 7.27	3.01 ± 0.36‡	59.60 ± 5.72	2.59 ± 0.27‡	68.10 ± 5.94	1.58 ± 0.19
Kenacort IVT	—	—	—	—	BLQ	21.65 ± 0.72

Table S1. Rabbit plasma exposure of SB568859 and plasma Lp-PLA_2 activity at days 4, 5, and 6 and following administration of 3–30 $mg \cdot kg^{-1} \cdot d^{-1}$ SB568859 by oral gavage

Male HY79b-pigmented rabbits were treated with SB568859 administered by mouth, at 0 (vehicle alone, n = 6), 3 (n = 6), 10 (n = 8), and 30 mg/kg, respectively, (n = 8) at each dose, once on day 1, twice (8 AM and 4 PM) on days 2–5, and once on day 6. Blood samples were collected on day 4 and day 5 (before the scheduled SB568859 dosing, equivalent to C_{trough}), and on day 6 (~2–3 h after the day 6 SB568859 dosing) for determination of SB568859 concentration and Lp-PLA_2 enzyme activity. Plasma was prepared by centrifugation at 13,000 x g and stored at −80 °C. SB568859 concentration was measured following protein precipitation by HPLC/MS/MS analysis. Lp-PLA_2 activity was evaluated by determining the enzyme-catalyzed release of [^{3}H-] acetate from 1-*O*-hexadecyl-2-*O*-[^{3}H-]acetyl-sn-glycer-3-phophorylcholine. BLQ, below level of quantitation; PO BID, by mouth, twice a day. * ng SB568859/ml rabbit plasma, mean ± standard deviation of the mean. † Lp-PLA2 enzyme rate (nmol/min/mL), mean ± standard deviation of the mean. ‡ Indicates n = 7.